Chemistry–A European Journal
Research Article
doi.org/10.1002/chem.202203806
Chemistry Europe
European Chemical Societies Publishing
www.chemeurj.org

Diverse Cooperative Reactivity at a Square Planar Aluminium Complex and Catalytic Reduction of CO_2

Chloe L. Shaves,[a] Nery Villegas-Escobar,[b] Ewan R. Clark,[c] and Ian M. Riddlestone*[a]

Abstract: The use of a sterically demanding pincer ligand to prepare an unusual square planar aluminium complex is reported. Due to the constrained geometry imposed by the ligand scaffold, this four-coordinate aluminium centre remains Lewis acidic and reacts via differing metal-ligand cooperative pathways for activating ketones and CO_2. It is also a rare example of a single-component aluminium system for the catalytic reduction of CO_2 to a methanol equivalent at room temperature.

Introduction

Metal ligand cooperativity (MLC) has been extensively used in transition metal-based homogeneous catalysis, enabling bond cleavage and formation steps without changing the metal oxidation state.[1–3] In cooperative reactions, the metal centre typically functions as a Lewis acid whilst acting with an electron-rich ligand site serving as a nucleophile. Pincer ligands are ideally suited to MLC as they allow for both coordinative control to stabilise a Lewis acidic metal centre and incorporate suitable functional groups to reversibly form the nucleophilic ligand site.[4] This process is often carried out through a secondary amine that can be de/(re)protonated, for example Macho-type scaffolds,[5] or a pyridine residue that can undergo dearomatisation/(re)aromatisation, for example Milstein's PNN- and PNP-scaffolds.[6]

MLC has facilitated the development of new highly efficient catalytic protocols and the application of base metals in catalysis.[7–9] Despite these successes in transition metal chemistry, metal (element) ligand cooperativity in main group chemistry remains rare.[10] This perhaps reflects the difficulties associated with the preparation of ambiphilic complexes featuring a Lewis acidic metal centre with a nucleophilic ligand site.

Structural constraint provides a method to manipulate frontier molecular orbitals and modify or enhance reactivity at a metal/element centre.[11–14] Examples of structurally constrained tetracoordinate (square planar) group 13 complexes are rare (Figure 1).[15–19] However, those reported remain appreciably Lewis acidic due to their unusual geometry and exhibit MLC reactivity.[20–25] We proposed that using an appropriate pincer ligand could induce Lewis acidity at aluminium by structural constraint and the formation of a nucleophilic ligand site to promote MLC reactivity.

We now report the use of a sterically demanding pincer ligand to impose structural constraint at an aluminium centre resulting in the formation of an unusual square planar aluminium complex. This square planar complex remains Lewis acidic and undergoes differing modes of metal-ligand cooperative reactivity with carbonyl-containing substrates, including

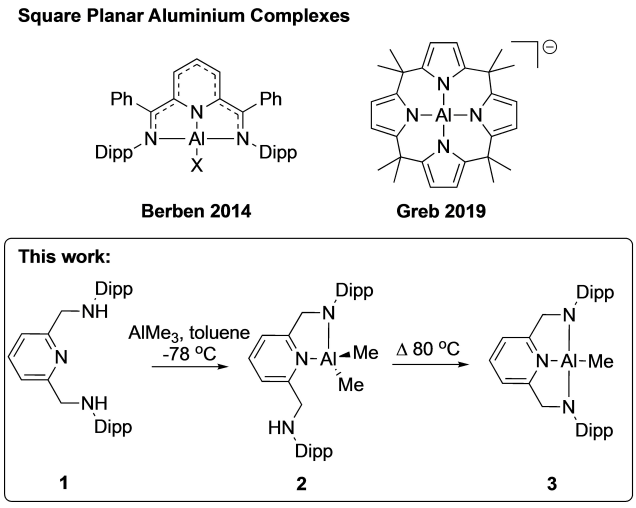

Figure 1. Previously reported examples of square planar aluminium complexes. X = H, Cl, and I (top); Synthesis of the new square planar aluminium complex **3** (bottom).

[a] *C. L. Shaves, Dr. I. M. Riddlestone*
Department of Chemistry
University of Surrey
Guildford, Surrey, GU2 7XH (UK)
E-mail: i.riddlestone@surrey.ac.uk
[b] *Dr. N. Villegas-Escobar*
Departamento de Físico-Química
Facultad de Ciencias Químicas
Universidad de Concepción
Concepción 4070386 (Chile)
[c] *Dr. E. R. Clark*
School of Physical Sciences
University of Kent
Canterbury, CT2 7NH (UK)

Supporting information for this article is available on the WWW under https://doi.org/10.1002/chem.202203806

CO_2. Furthermore, in the presence of pinacolborane (HBpin), it catalyses the room temperature reduction of CO_2 to the methanol equivalent MeOBpin.

Results and Discussion

The reaction of the sterically demanding NNN-pincer ligand **1** with $AlMe_3$ in toluene at low temperature, followed by warming to room temperature, results in the elimination of methane and the formation of the singly metalated complex **2** (Figure 1). Complex **2** has been characterised spectroscopically and by single-crystal X-ray diffraction (see Supporting Information). The elimination of the second equivalent of methane to form the doubly metalated complex **3** requires heating the toluene reaction mixture at 80 °C. Complex **3** was isolated as the toluene solvate by crystallisation at low temperature from toluene, and the molecular structure of **3**·0.5 toluene is shown in Figure 2.

The geometry at the aluminium centre of **3** is close to square planar, reflected by a τ_4 value of 0.20. This deviates from 0 predominantly due to the ligand-imposed distortion in the N(1)-Al(1)-N(3) angle (157.87(5)°) within the plane defined by the N(1), N(2), N(3), and C(1) centres. There are limited systems for comparison in the literature. However, the doubly reduced bis(imino) aryl-supported $^{Ph}I_2PAl$-X complexes reported by Berben (Figure 1) have τ_4 values of 0.22, 0.21 and 0.13 for X = Cl, I, and H, respectively.[15,16] The calix[4]pyrrolato aluminate system reported by Greb has a τ_4 value of 0.[17,18] The difference in electronic structure between the redox non-innocent $[^{Ph}I_2P]^{2-}$ ligand in $^{Ph}I_2PAl$–X and the precise electron bonding present in **3** is clearly illustrated by the comparison of Al–N bond distances. In **3**, the Al–N_{amide} bond distances (1.865(1) Å) are statistically indistinguishable and are considerably shorter than the Al–N_{Py} (2.008(1) Å). In contrast, in $^{Ph}I_2PAl$–X complexes, the Al–N_{Py} bond distance is shorter than the Al–N_{imine} (cf. Al–N_{Py} 1.820(1)-1.8331(9) Å; Al–N_{imine} 1.930(1)-1.965(5) Å) reflecting the reduction of the ligand scaffold and the amide donor character of the formerly pyridyl nitrogen.[15,16]

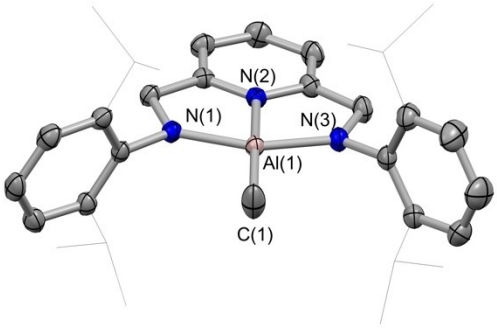

Figure 2. Molecular structure of **3** as determined by single-crystal X-ray diffraction. Thermal ellipsoids are set at the 40 % probability level. Hydrogen atoms and disordered toluene solvate are omitted, and the ^{i}Pr groups of the Dipp substituents are shown in wireframe for clarity. Selected bond distances (Å) and angles (°): Al(1)–N(1) 1.8650(9), Al(1)–N(2) 2.008(1), Al(1)–N(3) 1.865(1), Al(1)–C(1) 1.969(2); N(1)–Al(1)–N(2) 79.20(4), N(2)–Al-(1)–N(3) 78.98(4), N(2)–Al(1)–C(1) 174.48(6), N(1)–Al(1)–N(3) 157.87(5).

Complex **3** remains Lewis acidic, which was measured using the Gutmann-Beckett method.[26–28] Coordination of $Et_3P{=}O$ to **3** results in a $\Delta\delta_P = 17.0$ ppm indicating that **3** is a moderate Lewis acid, weaker than the $^{Ph}I_2PAl$-X complexes ($\Delta\delta = 23.2$ and 25.2 ppm for X = H and Cl respectively)[16] but similar to the calix[4]pyrrolato aluminate ($\Delta\delta = 17.0$ ppm).[17,29] The increased $^{31}P\{^{1}H\}$ NMR shift of the PhI_2PAl–X complexes is consistent with the calculated fluoride ion affinities, as discussed below.

To gain further insight into complex **3**, DFT calculations were performed. A plot of the Kohn-Sham frontier orbitals at the B3LYP–D3(BJ)/def2-TZVP level of theory shows that the HOMO predominantly relates to the N1 and N3 electron lone pairs (Figure 3) and the LUMO and LUMO + 1 are mostly ligand-based (see Supporting Information). However, the low-lying LUMO + 2 (−0.04 eV) shows significant localisation at aluminium consistent with **3** functioning as an aluminium based Lewis acid (Figure 3).

Whilst gas phase fluoride ion affinity (FIA) values for the calix[4]pyrrolato aluminate have been reported at the PW6B95-D3(BJ)/def2-TZVPP level of theory,[17] values for $^{Ph}I_2PAl$–X, have so far not been reported. The FIAs of **3** and $^{Ph}I_2PAl$-H were calculated using isodesmic reactions,[30] at this same level of theory, to be -370 and -390 kJ mol^{-1} respectively. They are significantly larger than those reported for the calix[4]pyrrolato aluminate (−128 kJ mol^{-1}), presumably reflecting their lack of negative charge.

Consistent with the presence of a vacant orbital at aluminium identified by computational studies, **3** functions as an aluminium-centred Lewis acid (natural charge Al 1.94 | e |). In contrast to typical aluminium-based organometallics, the Al–Me bond does not react with ketones (cf. $AlMe_3$). In fact, probing the coordination of substrates to **3** with ketones identified alternative reactivity consisting of differing modes of MLC (Scheme 1). The addition of the non-enolisable ketone benzophenone to a solution of **3** in C_6D_6 immediately results in the oxidation of the ligand scaffold and transfer of a hydride from

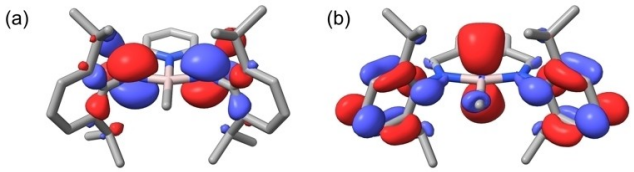

Figure 3. Kohn-Sham frontier orbital plots of the HOMO (a) and LUMO + 2 (b) at the B3LYP–D3(BJ)/def2-TZVP level of theory.

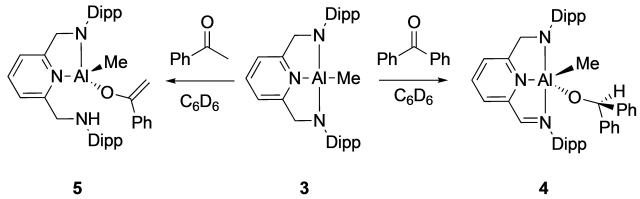

Scheme 1. Contrasting metal-ligand cooperative reactivity of **3** with enolisable and non-enolisable ketones.

the methylene group of the ligand to the benzophenone.[31] The resulting imine and corresponding aluminium-bound alkoxide are readily identified from the ^{1}H NMR spectrum of **4**. Reactivity with the more sterically demanding fluorenone proceeded more slowly but gave the analogous product.

In contrast, the addition of the enolisable ketone acetophenone to a C_6D_6 sample of **3** results in the immediate deprotonation by one of the aluminium amides and formation of the aluminium enolate **5** (Scheme 1). This is evidenced by the ^{1}H NMR spectrum, where the alkenyl protons are observed as singlets, each integrating to 1 at $\partial_H = 4.69$ and 3.91 ppm. In addition, the secondary amine proton and the adjacent methylene protons are mutually coupled, resulting in an ABX splitting pattern. The crystallisation of **4** and **5** proved elusive, but further confirmation of this reactivity was achieved through controlled degradation studies (see Supporting Information).

Exposing a degassed solution of **3** in dichloromethane to CO_2 (1 bar) resulted in the formation of a small amount of precipitate and a pale-yellow solution. Filtration and subsequent crystallisation resulted in the characterisation of the dimer **6**. CO_2 inserts into the Al–N_{amide} bond, forming a carbamate (**6$_M$** in Figure 4). Two of these units dimerise, resulting in a thermodynamically favoured pentacoordinate aluminium centre with distorted trigonal bipyramidal geometry (Figure 5) ($\Delta\Delta G^\circ = -33.6$ kcal mol^{-1}).

Whilst the insertion of CO_2 into Al–N bonds has been reported,[32–34] comparisons can be drawn between the reactivity of **3** towards CO_2 and that of transition metal pincer complexes featuring an amide donor.[35,36] The dimeric nature of **6** in the solid state highlights the greater oxophilicity of aluminium which drives dimerisation and bridging, rather than κ^2-N,O-bound carbamate groups.

To gain greater insight into the differing modes of reactivity between carbonyl-containing substrates, we turned to DFT. The

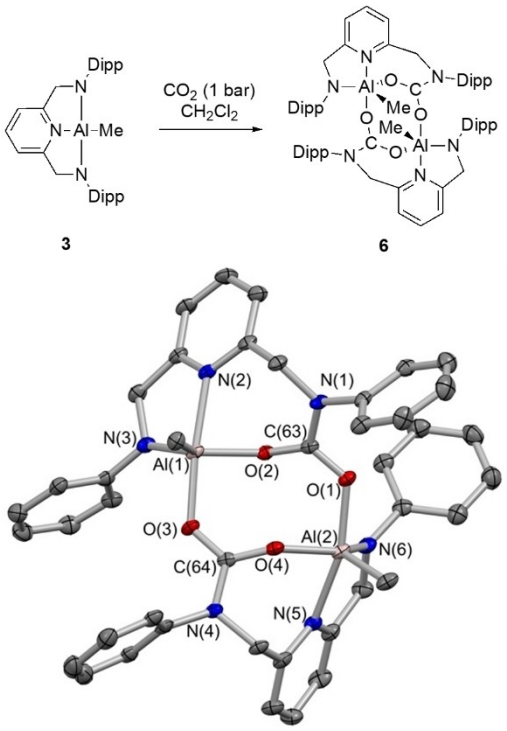

Figure 5. Reactivity of **3** with CO_2 in dichloromethane solution (top); Molecular structure of **6** as determined by single-crystal X-ray diffraction. Thermal ellipsoids set at the 40% probability level. Hydrogen atoms, dichloromethane solvate and the ^{i}Pr groups of the Dipp substituents are omitted for clarity. Selected bond distances (Å) and angles (°): Al(1)–O(2) 1.845(3), Al(1)–O(3) 1.934(2), C(63)–O(1) 1.271(4), C(63)–O(2) 1.265(4), Al(2)–O(1) 1.907(2), Al(2)–O(4) 1.844(3), C(64)–O(3) 1.270(4), C(64)–O(4) 1.260(4); N(2)–Al(1)–O(3) 168.85(11), N(1)–C(63)–O(1) 116.8(3), O(1)–C(63)–O-O(2) 123.5(3), O(2)–C(63)–N(1) 119.6(3), N(5)–Al(2)–O(1) 162.40(12), N-(4)–C(64)–O(3) 119.4(3), O(3)–C(64)–O(4) 124.1(3), O(4)–C(64)–N(4) 116.5(3).

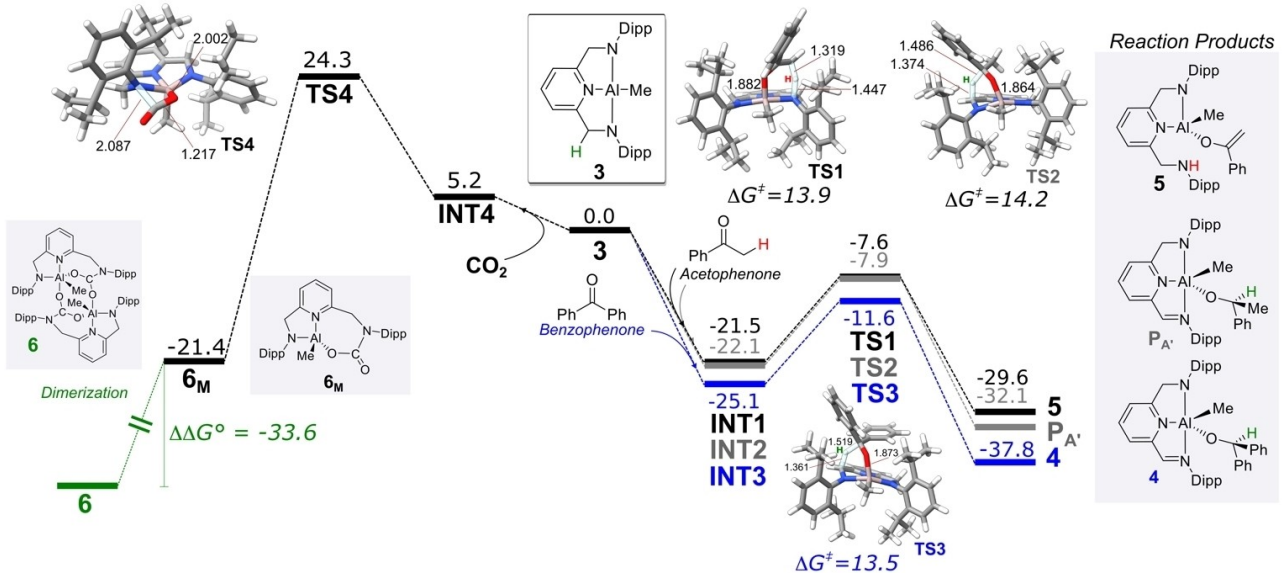

Figure 4. Computed reaction profile (free energy, kcal mol^{-1}) for the reactions of **3** with acetophenone, benzophenone and CO_2. Computed geometries for key transition states are shown with bond distances in Å.

energy profiles for the reactions of **3** with benzophenone, acetophenone, and CO_2 were computed at the B3LYP-D3(BJ)/def2-TZVP level of theory. The reaction profiles, including solvent effects, are shown in Figure 4. The Lewis acidity of aluminium is central to this reactivity, and the first step in each reaction is the coordination of the substrate oxygen atom to aluminium. For acetophenone (**INT1**) and benzophenone (**INT3**), these intermediates are stabilised by −21.5 and −25.1 kcal mol^{-1}, and the binding of CO_2 (**INT4**) is only thermodynamically uphill by +5.2 kcal mol^{-1}. Transition states were located for the reactions with acetophenone (**TS1**), benzophenone (**TS3**), and CO_2 (**TS4**), corresponding to overall reaction barriers of 13.9, 13.5, and 24.3 kcal mol^{-1}, respectively. Although the Gibbs free energy of activation for **TS4** is relatively high, attempts to identify alternative pathways involving a dimer of **3** or concerted CO_2 activation were unsuccessful. Interestingly, the difference in reaction barrier for the reduction of acetophenone (**INT2** to **TS2**) was only marginally higher in energy (14.2 kcal mol^{-1}) than that for the experimentally observed deprotonation (13.9 kcal mol^{-1}).

With the coordination of the carbonyl fragment to the Lewis acidic aluminium centre proving crucial to the reactivity of **3**, its potential toward hydroboration catalysis was investigated. Whilst **3** functions as a modest hydroboration catalyst for ketones and esters (TOFs of 0.38–2.10 h^{-1}) (see Supporting Information), the addition of CO_2 (1 bar) to a CD_2Cl_2 solution of **3** (5 mol%) and HBpin results in the room temperature catalytic reduction of CO_2. Monitoring of the reaction by multinuclear NMR spectroscopy identifies the final products of the reduction as the methanol equivalent MeOBpin and pinBOBpin (Scheme 2).

Although complete conversion of HBpin does not occur even at extended reaction times (5 days) **3** has a TOF of 0.08 h^{-1} (see Supporting Information). It therefore falls within the range of other reported main group systems for CO_2 hydroboration (0.07-14.5 h^{-1}),[37–42] but is a rare example of a single component system[43] operating at room temperature with HBpin as the reducing agent.[23,39,42] To our knowledge, the only other example based on aluminium is the square planar calix[4]pyrrolato aluminate reported by Greb (TOF = 0.12 h^{-1}).[23] The catalytic hydroboration reactivity of **3** contrasts the properties of the β-diketiminate aluminium hydride complexes reported by Aldridge, for which catalytic turnover is unfavourable.[44]

Conclusion

In conclusion, the use of the sterically demanding pincer ligand **1** allows for the synthesis of the structurally constrained compound **3** as an unusual square-planar Al^{III} complex. Due to its geometry, **3** is Lewis acidic at Al and this, in combination with the electron-rich ligand scaffold, results in multiple metal-ligand cooperative bond activation modes with carbonyl-containing small molecules. This reactivity can be exploited by using the borane HBpin to allow for the catalytic hydroboration of CO_2, reducing it to a methanol equivalent. Further studies on the mechanism of catalysis and extension of this cooperative reactivity are ongoing.

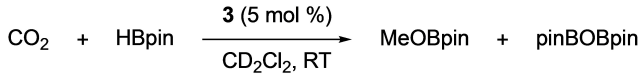

Scheme 2. Room temperature catalytic hydroboration of CO_2 by **3**.

Experimental Section

General considerations: All manipulations were carried out under an atmosphere of argon or dinitrogen using standard Schlenk line and glove box techniques. Prior to use all solvents were dried and stored over activated molecular sieves or a potassium mirror. 2,6-di*iso*propylaniline was vacuum distilled from CaH_2 and stored over activated molecular sieves. Acetophenone was vacuum transferred from CaH_2 and stored over activated molecular sieves. Benzophenone and 9-fluorenone were dried in vacuo with P_2O_5 for 3 days. All other reagents were used as received from the supplier. NMR spectra were recorded on Bruker Ascend 400 MHz and Bruker Avance III 500 MHz spectrometers and referenced to residual solvent signals for ^{1}H and ^{13}C spectra for C_6D_6 (δ 7.16, 128.06), CD_2Cl_2 (δ 5.32, 53.84) and C_7D_8 (δ 2.08). Detailed experimental and computational methods can be found in the Supporting Information.

[MeAl(Py(CH$_2$NDipp)$_2$)]·xToluene (**3**): To a solution of **1** (3.375 g, 7.37 mmol) in toluene (60 cm^3) at −90 °C $AlMe_3$ (4 cm^3 of 2.0 M in hexanes, 8 mmol) was added slowly and the reaction mixture was stirred for 16 h whilst slowly attaining room temperature. The reaction mixture was then heated at 80 °C for 79.5 h. The resulting solution was concentrated and cooled to −20 °C yielding yellow crystals of **3**. Further crops of **3** were obtained from concentration of the mother liquor and cooling to −20 °C. **3** was isolated as a solvate **3**·0.4–0.6toluene. Yield: 2.671 g, 67%. ^{1}H NMR (400 MHz, C_6D_6, 298 K): δ 7.21 (s, 6H, Ar*H*), 6.86 (t, $^3J_{HH}$ = 7.7 Hz, 1H, *p*-Py*H*), 6.39 (d, $^3J_{HH}$ = 7.7 Hz, 2H, *m*-Py*H*), 4.27 (s, 4H, CH_2), 3.61 (sept, $^3J_{HH}$ = 6.9 Hz, 4H, ^{i}PrC*H*), 1.33 (br s, 24H, ^{i}PrCH_3), −0.79 (s, 3H, CH_3). ^{13}C{^{1}H} NMR (101 MHz, C_6D_6, 298 K): δ 158.8 (*o*-PyC), 148.0 (*ipso*-ArC), 146.7 (*o*-ArC), 138.4 (*p*-PyC), 125.0 (ArC), 123.9 (ArC), 118.5 (*m*-PyC), 56.9 (CH_2), 28.1 (^{i}PrCH), 26.1 (^{i}PrCH_3), 24.8 (^{i}PrCH_3), −9.1 (CH_3). ^{1}H NMR (500 MHz, C_7D_8, 243 K): δ 7.18 (s, 6H, Ar*H*), 6.79 (t, $^3J_{HH}$ = 7.7 Hz, 1H, *p*-Py*H*), 6.29 (d, $^3J_{HH}$ = 7.7 Hz, 2H, *m*-Py*H*), 4.20 (s, 4H, CH_2), 3.60 (sept, $^3J_{HH}$ = 6.9 Hz, 4H, ^{i}PrC*H*), 1.35 (d, $^3J_{HH}$ = 6.9 Hz, 12H, ^{i}PrCH_3), 1.31 (d, $^3J_{HH}$ = 6.9 Hz, 12H, ^{i}PrCH_3), −0.84 (s, 3H, CH_3). Anal. Calcd for $C_{32}H_{44}AlN_3$·0.46toluene: C 78.32, H 8.9, N 7.78; found C 78.02, H 8.94, N 7.42.

[{Me(μ-OCO)Al(Py(CH$_2$NDipp)$_2$)}$_2$]·0.15DCM (**6**): A solution of **3** (0.504 g, 0.93 mmol) in DCM (20 cm^3) was freeze-pump-thaw degassed four times and then filled with CO_2 (1 bar). The resulting solution was left to stir at rt for 21 h yielding a yellow solution with a white precipitate floating on top. The reaction mixture was filtered, and the filtrate was concentrated and cooled to −20 °C yielding colourless crystals of **6**. Further crops of **6** were obtained from concentration of the mother liquor. The isolated precipitate was also dried in vacuo to give a **6** as a white solid. Yield: 0.0951 g, 19%.^{1}H NMR (400 MHz, CD_2Cl_2, 298 K): δ 7.71 (t, $^3J_{HH}$ = 7.7 Hz, 1H, *p*-Py*H*), 7.16 (m, 4H, Ar*H*), 6.98 (m, 1H, Ar*H*), 6.85 (m, 3H, Ar*H*), 5.75 (d, $^2J_{HH}$ = 14.0 Hz, 1H, CH_2), 4.09 (s, 2H, CH_2), 3.71 (d, $^2J_{HH}$ = 14.0 Hz, 1H, CH_2), 3.58 (sept, $^3J_{HH}$ = 6.9 Hz, 1H, ^{i}PrC*H*), 3.42 (sept, $^3J_{HH}$ = 6.9 Hz, 1H, ^{i}PrC*H*), 3.24 (sept, $^3J_{HH}$ = 6.7 Hz, 1H, ^{i}PrC*H*), 2.57 (sept, $^3J_{HH}$ = 6.8 Hz, 1H, ^{i}PrC*H*), 1.51 (d, $^3J_{HH}$ = 6.8 Hz, 6H, ^{i}PrCH_3), 1.27 (d, $^3J_{HH}$ = 6.8 Hz, 6H, ^{i}PrCH_3), 1.18 (d, $^3J_{HH}$ = 6.9 Hz, 6H, ^{i}PrCH_3), 1.08 (d, $^3J_{HH}$ = 6.8 Hz, 6H,

^{i}PrCH_3), 1.01 (d, $^3J_{HH}$ = 6.9 Hz, 6H, ^{i}PrCH_3), 0.53 (d, $^3J_{HH}$ = 6.8 Hz, 6H, ^{i}PrCH_3), 0.42 (d, $^3J_{HH}$ = 6.7 Hz, 6H, ^{i}PrCH_3), 0.12 (d, $^3J_{HH}$ = 6.7 Hz, 6H, ^{i}PrCH_3), −0.80 (s, 3H, CH_3). ^{13}C{^{1}H} NMR (101 MHz, CD_2Cl_2, 298 K): δ 160.7 (*o*-PyC), 159.4 (OC(O)N), 152.5 (*o*-PyC), 149.9 (ArC), 148.4 (ArC), 148.1 (ArC), 147.0 (ArC), 146.9 (ArC), 139.5 (ArC), 138.2 (*p*-PyC), 128.4 (ArC), 124.2 (ArC), 124.1 (ArC), 124.1 (ArC), 124.0 (ArC), 123.9 (ArC), 123.7 (ArC), 121.1 (ArC), 60.9 (CH_2), 56.5 (CH_2), 28.8 (^{i}PrCH), 28.3 (^{i}PrCH), 27.4 (^{i}PrCH_3), 26.9 (^{i}PrCH), 26.8 (^{i}PrCH), 25.6 (^{i}PrCH_3), 25.1 (^{i}PrCH_3), 25.0 (^{i}PrCH_3), 25.0 (^{i}PrCH_3), 23.9 (^{i}PrCH_3), 23.4 (^{i}PrCH_3).IR (CH_2Cl_2, cm^{-1}): 1606 (ν_{CO}). Anal. Calcd for $C_{33}H_{44}AlN_3O_2$.0.15CH_2Cl_2: C 71.81, H 8.05, N 7.58; found C 71.86, H 8.12, N 7.32.

General procedure for ketone and ester hydroboration: The substrate (0.4 mmol), HBpin (0.44 mmol, 1.1 equiv.), and 1,3,5-trimethoxybenzene (10 mol%) were dissolved in C_6D_6 (0.5 cm^3) and added to **3** (5 mol%). The resulting solution was immediately transferred into a J Young's NMR tube and the ^{1}H and ^{11}B NMR spectra were recorded immediately and then periodically whilst maintained at room temperature.

General procedure for CO_2 hydroboration: In a J Young's NMR tube, HBpin (0.4 mmol) and 1,3,5-trimethoxybenzene (25 mol%) were dissolved in CD_2Cl_2 (0.3 cm^3). A solution of **3** (5 mol%) in CD_2Cl_2 (0.4 cm^3) was further added to the NMR tube. The solution was freeze-pump-thaw degassed four times and then filled with CO_2 (1 bar). The ^{1}H and ^{11}B NMR spectra were recorded immediately and then periodically whilst maintained at room temperature.

Deposition Numbers 2211657 (**2**), 2211658 (**3**), and 2211659 (**6**) contain the supplementary crystallographic data for this paper. These data are provided free of charge by the joint Cambridge Crystallographic Data Centre and Fachinformationszentrum Karlsruhe Access Structures service.

DFT calculations: Calculations were carried out using either Orca 4.2.0[45–47] or the Gaussian16[48] software packages. Geometries were fully optimised and confirmed to be true minima on the respective potential energy surfaces.

Acknowledgements

We acknowledge the University of Surrey for supporting this work and a studentship (CS). NVE acknowledges the financial support of ANID-Postdoctorado Grant N 3210532. This research was supported by the high-performance computing system of PIDi-UTEM (SCC-PIDi-UTEM FONDEQUIP-EQM180180).

Conflict of Interest

The authors declare no conflict of interest.

Data Availability Statement

The data that support the findings of this study are available in the supplementary material of this article.

Keywords: aluminium · carbon dioxide · cooperativity · Lewis acid · structural constraint

[1] J. R. Khusnutdinova, D. Milstein, *Angew. Chem. Int. Ed.* **2015**, *54*, 12236–12273; *Angew. Chem.* **2015**, *127*, 12406–12445.
[2] H. Grützmacher, *Angew. Chem. Int. Ed.* **2008**, *47*, 1814–1818; *Angew. Chem.* **2008**, *120*, 1838–1842.
[3] T. Higashi, S. Kusumoto, K. Nozaki, *Chem. Rev.* **2019**, *119*, 10393–10402.
[4] M. A. W. Lawrence, K. A. Green, P. N. Nelson, S. C. Lorraine, *Polyhedron* **2018**, *143*, 11–27.
[5] S. Schneider, J. Meiners, B. Askevold, *Eur. J. Inorg. Chem.* **2012**, 412–429.
[6] D. Milstein, *Phil. Trans. R. Soc. A.* **2015**, *373*, 20140189.
[7] M. R. Elsby, R. Tom Baker, *Chem. Soc. Rev.* **2020**, *49*, 8933.
[8] A. Kumar, D. Milstein, *Top. Organomet. Chem.* **2021**, *68*, 1–24.
[9] L. Alig, M. Fritz, S. Schneider, *Chem. Rev.* **2018**, *119*, 2681–2751.
[10] L. Greb, F. Ebner, Y. Ginzburg, L. M. Sigmund, *Eur. J. Inorg. Chem.* **2020**, 3030–3047.
[11] S. Culley, A. J. Arduengo, *J. Am. Chem. Soc.* **1984**, *106*, 1164–1165.
[12] J. C. Gilhula, A. T. Radosevich, *Chem. Sci.* **2019**, *10*, 7177–7182.
[13] T. P. Robinson, D. M. de Rosa, S. Aldridge, J. M. Goicoechea, *Angew. Chem. Int. Ed.* **2015**, *54*, 13758–13763; *Angew. Chem.* **2015**, *127*, 13962–13967.
[14] N. L. Dunn, M. Ha, A. T. Radosevich, *J. Am. Chem. Soc.* **2012**, *134*, 11330–11333.
[15] E. J. Thompson, T. W. Myers, L. A. Berben, *Angew. Chem. Int. Ed.* **2014**, *53*, 14132–14134; *Angew. Chem.* **2014**, *126*, 14356–14358.
[16] T. M. Bass, C. R. Carr, T. J. Sherbow, J. C. Fettinger, L. A. Berben, *Inorg. Chem.* **2020**, *59*, 13517–13523.
[17] F. Ebner, H. Wadepohl, L. Greb, *J. Am. Chem. Soc.* **2019**, *141*, 18009–18012.
[18] F. Ebner, P. Mainik, L. Greb, *Chem. Eur. J.* **2021**, *27*, 5120–5124.
[19] L. M. Sigmund, E. Engels, N. Richert, L. Greb, *Chem. Sci.* **2022**, *13*, 11215.
[20] L. A. Berben, *Chem. Eur. J.* **2015**, *21*, 2734–2742.
[21] T. W. Myers, L. A. Berben, *Chem. Sci.* **2014**, *5*, 2771–2777.
[22] T. W. Myers, L. A. Berben, *J. Am. Chem. Soc.* **2013**, *135*, 9988–9990.
[23] F. Ebner, L. M. Sigmund, L. Greb, *Angew. Chem. Int. Ed.* **2020**, *59*, 17118–17124; *Angew. Chem.* **2020**, *132*, 17266–17272.
[24] L. M. Sigmund, L. Greb, *Chem. Sci.* **2020**, *11*, 9611–9616.
[25] L. M. Sigmund, C. Ehlert, M. Enders, J. Graf, G. Gryn'ova, L. Greb, *Angew. Chem. Int. Ed.* **2021**, *60*, 15632–15640; *Angew. Chem.* **2021**, *133*, 15761–15769.
[26] M. A. Beckett, G. C. Strickland, J. R. Holland, K. S. Varma, *Polymer* **1996**, *37*, 4629–4631.
[27] U. Mayer, V. Gutmann, W. Gerger, *Monatsh. Chem.* **1975**, *106*, 1235–1257.
[28] G. C. Welch, L. Cabrera, P. A. Chase, E. Hollink, J. D. Masuda, P. Wei, D. W. Stephan, *Dalton Trans.* **2007**, 3407.
[29] P. Erdmann, L. Greb, *Angew. Chem. Int. Ed.* **2022**, *61*, e202114550.
[30] P. Erdmann, J. Leitner, J. Schwarz, L. Greb, *ChemPhysChem* **2020**, *21*, 987–994.
[31] O. T. Summerscales, J. A. Stull, B. L. Scott, J. C. Gordon, *Inorg. Chem.* **2015**, *54*, 6885–6890.
[32] W. Haider, M. D. Calvin-Brown, I. A. Bischoff, V. Huch, B. Morgenstern, C. Müller, T. Sergeieva, D. M. Andrada, A. Schäfer, *Inorg. Chem.* **2022**, *61*, 1672–1684.
[33] F. Hengesbach, X. Jin, A. Hepp, B. Wibbeling, E. U. Würthwein, W. Uhl, *Chem. Eur. J.* **2013**, *19*, 13901–13909.
[34] A. R. Kennedy, R. E. Mulvey, D. E. Oliver, S. D. Robertson, *Dalton Trans.* **2010**, 6190–6197.
[35] S. Chakraborty, O. Blacque, H. Berke, *Dalton Trans.* **2015**, *44*, 6560.
[36] A. Kumar, P. Daw, N. A. Espinosa-Jalapa, G. Leitus, L. J. W. Shimon, Y. Ben-David, D. Milstein, *Dalton Trans.* **2019**, *48*, 14580–14584.
[37] M. D. Anker, M. Arrowsmith, P. Bellham, M. S. Hill, G. Kociok-Kohn, D. J. Liptrot, M. F. Mahon, C. Weetman, *Chem. Sci.* **2014**, *5*, 2826–2830.
[38] J. A. B. Abdalla, I. M. Riddlestone, R. Tirfoin, S. Aldridge, *Angew. Chem. Int. Ed.* **2015**, *54*, 5098–5102; *Angew. Chem.* **2015**, *127*, 5187–5191.
[39] T. J. Hadlington, C. E. Kefalidis, L. Maron, C. Jones, *ACS Catal.* **2017**, *7*, 1853–1859.
[40] D. Franz, C. Jandl, C. Stark, S. Inoue, *ChemCatChem* **2019**, *11*, 5275.
[41] C.-C. Chia, Y.-C. Teo, N. Cham, S. Ying-Fu Ho, Z.-H. Ng, H.-M. Toh, N. Mézailles, C.-W. So, *Inorg. Chem.* **2021**, *60*, 4569–4577.
[42] L. Liu, S.-K. Lo, C. Smith, J. M. Goicoechea, *Chem. Eur. J.* **2021**, *27*, 17379–17385.
[43] C. Ni, X. Ma, Z. Yang, H. W. Roesky, *Eur. J. Inorg. Chem.* **2022**, e202100929.
[44] A. Caise, D. Jones, E. L. Kolychev, J. Hicks, J. M. Goicoechea, S. Aldridge, *Chem. Eur. J.* **2018**, *24*, 13624.
[45] F. Neese, *Wiley Interdiscip. Rev.: Comput. Mol. Sci.* **2012**, *2*, 73–78.

[46] F. Neese, *Wiley Interdiscip. Rev.: Comput. Mol. Sci.* **2018**, *8*, 10.1002/WCMS.1327.
[47] F. Neese, F. Wennmohs, U. Becker, *J. Chem. Phys.* **2020**, *152*, 224108.
[48] M. J. Frisch, G. W. Trucks, H. B. Schlegel, G. E. Scuseria, M. A. Robb, J. R. Cheeseman, G. Scalmani, V. Barone, G. A. Petersson, H. Nakatsuji, X. Li, M. Caricato, A. V. Marenich, J. Bloino, B. G. Janesko, R. Gomperts, B. Mennucci, H. P. Hratchian, J. V. Ortiz, A. F. Izmaylov, J. L. Sonnenberg, D. Williams-Young, F. Ding, F. Lipparini, F. Egidi, J. Goings, B. Peng, A. Petrone, T. Henderson, D. Ranasinghe, V. G. Zakrzewski, J. Gao, N. Rega, G. Zheng, W. Liang, M. Hada, M. Ehara, K. Toyota, R. Fukuda, J. Hasegawa, M. Ishida, T. Nakajima, Y. Honda, O. Kitao, H. Nakai, T. Vreven, K. Throssell, J. Montgomery, J. A., J. E. Peralta, F. Ogliaro, M. J. Bearpark, J. J. Heyd, E. N. Brothers, K. N. Kudin, V. N. Staroverov, T. A. Keith, R. Kobayashi, J. Normand, K. Raghavachari, A. P. Rendell, J. C. Burant, S. S. Iyengar, J. Tomasi, M. Cossi, J. M. Millam, M. Klene, C. Adamo, R. Cammi, J. W. Ochterski, R. L. Martin, K. Morokuma, O. Farkas, J. B. Foresman, D. J. Fox, *Gaussian 16, Revis. B.01*, **2016**, *Gaussian, Inc.: Wallingford, CT*.

Manuscript received: December 6, 2022
Accepted manuscript online: December 13, 2022
Version of record online: ■■, ■■■

RESEARCH ARTICLE

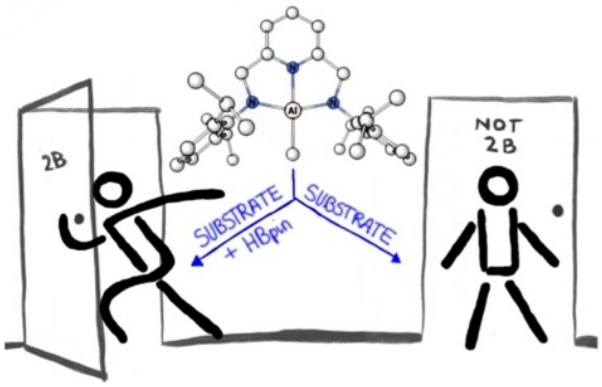

*C. L. Shaves, Dr. N. Villegas-Escobar, Dr. E. R. Clark, Dr. I. M. Riddlestone**

Structural constraint imparted by a sterically demanding pincer ligand results in an unusual tetracoordinate aluminium Lewis acid that undergoes multiple modes of metal-ligand cooperative reactivity with ketones and CO_2. Adding HBpin allows for the catalytic hydroboration of carbonyl-containing substrates and the reduction of CO_2 to a methanol equivalent.